Theor Chim Acta (1993) 86: 297–313

Theoretica Chimica Acta

Equivariant Morse theory of the N-body problem: Application to potential surfaces in chemistry

Daniel Liotard[1] and Michel Rérat[2]

[1] Laboratoire de Physico-Chimie Théorique, Université de Bordeaux I, F-33405 Talence, France

[2] Laboratoire de Chimie Structurale, Université de Pau, F-64000 Pau, France

Received August 13, 1990/Accepted December 29, 1992

Summary. The Morse inequalities linking the critical points of a potential function on the whole configuration space and its restrictions to either planar or linear configurations are derived from the Morse theory in its equivariant form. Brute potential functions arising from standard models of quantum chemistry need eventually morsification which can be achieved without altering the main chemical significances of the potential. Illustrative applications follow in the case of magnesium clusters.

Key words: Morse theory – Potential surfaces – Magnesium clusters

1. Introduction

A consequence of the Born–Oppenheimer approximation [1], the concept of potential energy hypersurface is a fundamental one in chemistry. The term "hypersurface" is to be understood as the graph of some potential function (the energy) of the $3N$ coordinates of the N nuclei of a molecular system. In the absence of external field, the energy depends only on the interatomic distances and its invariant under a translation/rotation/reflexion of the system as a whole. In spite of the energy arising numerically from various models (analytical form, SCF + CI, effective hamiltonian, etc.) we can assume conveniently the potential function to be an eigenvalue (usually the lowest one) of some hamiltonian matrix the elements of which being implicitly smooth functions of the interatomic distances. Removing the translational/rotational degrees of freedom, one obtains the configuration space (CS, defined precisely in the following section) in which the main properties of a potential function are primarily summarized in terms of its critical points.

At a critical point on CS, the potential function is at a stationary value. The behavior of the potential in a neighborhood of such a point is usually dominated by the second-order terms of a Taylor expansion, i.e. the hessian matrix, the signs of the eigenvalues of which usually characterize the nature of the critical point. Defining the index of a critical point as the number of strictly negative eigenvalues of the hessian, one gets a brief characterization of any kind of critical point. Chemically stable species correspond to minima (critical points with index

zero) while transition structures correspond to saddle points (critical points with index one). The potential function turns out to be smooth almost everywhere and usually exhibits non degenerate critical values (i.e. no zero eigenvalues of the hessian at a critical point). As a consequence, a potential function in chemistry usually belongs to the generic class of the so-called Morse functions and the Morse theory [2] does apply to large parts of the configuration space. More precisely let $f: \mathscr{R}^n \to \mathscr{R}$ be a Morse function on a simply connected domain X of $\mathscr{R}^n$ with (possibly empty) boundary B such that

(i) f is bounded below,
(ii) for each x in B, the gradient vector points out of X,

then the following inequalities hold:

$$M_k \geqslant \beta_k \quad (k = 0, \ldots, n)$$

and

$$M_k - M_{k-1} + \cdots + (-1)^k M_0 \geqslant \beta_k - \beta_{k-1} + \cdots + (-1)^k \beta_0$$

where M_k is the number of critical points with index k of the function f in X and β_k is the Betti number of rank k of X. Moreover the equality holds when k reaches n, the dimension of X. The Betti numbers are topological invariants of X and have been computed for usual topological spaces [3, 4] such as the n-dimensional balls $\mathscr{R}^n$, spheres $\mathscr{S}^n$, torus Π^n or direct products of such spaces. A condition on boundary, more precise than (ii), can be found in [5].

These relations can be used as diagnosis for completeness of the set of critical points at any stage of a numerical prospection restricted to any kind of domain X where the Morse theory holds. If any of these relations is violated, then there must exist some additional critical points with definite indices in X. Combining interrelated subdomains provided by symmetry constrained cross-sections, one obtains a severe check on the coherence in the course of a numerical approach to a potential function in chemistry as pointed out earlier by P. Mezey [6] and one of us [7]. Actual applications can be found elsewhere, either in $\mathscr{R}^n$ [8] or in Π^n [9]. For a recent survey of topological methods in chemistry including Morse theory in relation to potential surfaces, see [10]. However, one must keep in mind that a potential function in chemistry does not fall automatically into the field covered by the original Morse theory. Five difficulties can be pointed out. They are:

1. asymptotic behavior not satisfying condition (ii), as observed with more or less repulsive potentials.
2. first order discontinuity such as conical intersections on adiabatic potentials,
3. appearance of degenerate critical values (vanishing eigenvalues of the hessian),
4. pathological configurations where at least two atoms are superimposed,
5. appearance of degenerate critical orbits coming from the rotational equivalences.

The first three difficulties can be circumvented by using standard mathematical techniques (penalization, regularization, bifurcation) as proposed in [10, 15, 16] and summarized in appendix 1. The result is the formal and numerical replacement of the original potential V by a morsified one with smooth properties everywhere. In so doing, chemical significances of V are not altered due to the one-to-one correspondence between the topological properties of both origi-

nal and morsified functions. Following P. Mezey [10, 11], the difficulty (4) may usually be circumvented by a smoothing of the potential function in the vicinity of $D_{\text{excl.}}$, the set of pathological configurations.

The aim of this work is to write the Morse inequalities for a morsified potential function on the configuration space as a whole. We first tried the compacification method suggested by P. Mezey, but we encountered major difficulties in the four body cases. Details are given in appendix 2 where are quoted some obstacles at the compacification of the whole configuration space of a N-body problem ($N > 3$).

In the course of the following sections, the difficulty (4) will be overcome in the spirit of [12] and using the behavior of a chemical potential in the vicinity of such configurations. We will take advantage from recent progress about the central configurations of the N-body problem via equivariant Morse theory [13, 14] to solve the difficulty (5). The approach also yields Morse inequalities on the restrictions of the configuration space to either the planar or the collinear configurations.

2. Morse theory on the configuration space as a whole

Let $V(q_1, \ldots, q_n)$ be a Morsified potential function of a set of N nuclei with cartesian coordinates q_i and masses μ_i. The configuration space (CS) is derived from $\mathscr{R}^n$ in the following way:

(a) omission (by excision) of $D_{\text{excl.}}$, the set of configurations with two or more superimposed nuclei,
(b) elimination (by mapping) of the 3 translational degrees of freedom.
(c) elimination (by quotient) of the 2 or 3 rotational degrees of freedom

$$D_{ij} = \{(q_1, \ldots, q_n) \in \mathscr{R}^{3N}, i \neq j: q_i = q_j\}, \quad D_{\text{excl.}} = \bigcup_{i<j} D_{ij}$$

$$\left\{\mathscr{R}^{3N} \backslash D_{\text{excl.}}, \sum_{i=1}^{N} \mu_i q_i = 0\right\} = M, \quad M \backslash SO(3) = CS$$

Here M comes from the mapping which translates the center of mass at the origin and $SO(3)$ is the rotation group in $\mathscr{R}^3$ (not rotation-reflexion). When omitting $D_{\text{excl.}}$, the difficulty (4) is circumvented but M is not compact. This is not an obstacle because the critical points of V are bounded away from the set $D_{\text{excl.}}$: from the repulsion between nuclei, namely $V(q) \to \infty$ as $q \to 0$ (see also [11]). The space M turns out to be a $3N-3$ dimensional manifold. However M is no longer homotypically equivalent to $\mathscr{R}^{3N-3}$ due to the excision of $D_{\text{excl.}}$ and relevant Betti numbers are needed to pursue. Fortunately, such "configuration spaces" have been studied [12] and the homotopy of M is given by

$$P_M(t) = (1+t^2)(1+2t^2)\cdots(1+(N-1)t^2) = \sum_{i=0}^{N-1} \beta_i^{(N)} t^{2i} \tag{1}$$

where $P_M(t)$ is the Poincaré polynomial in t and $\beta_i^{(N)}$ are the Betti numbers of M.

The set of critical points of V on M defines two or three-dimensional critical orbits due to the rotational degrees of freedom. These orbits reduce to isolated critical points on CS, the quotient space of M by the group $SO(3)$. Unfortunately, $SO(3)$ does not act freely[1] on M and CS fails to be a manifold, a

[1] A group G acts freely on a space X if one has: $\forall x \in X$, $\forall g \in G$, $g \neq 1 \Rightarrow gx \neq x$.

necessary condition for the original Morse theory to apply. However the equivariant form of the Morse theory does apply on M, but the cohomology of the critical orbits needs to be explicited. A similar problem has been recently studied with the gravity law being the N body potential function [13]. The equivariant form of the Morse theory takes the form:

$$\sum_{j=1}^{n} t^{\lambda_j} P_j(t) = \frac{P_M(t)}{1-t^4} + (1+t)Q_V(t) \tag{2}$$

where the sum on the left hand side runs over the critical orbits of V on M, λ_j is the index of the hessian restricted on the space transverse to the orbit j and $P_j(t)$ is a series in t which represents the equivariant cohomology of the orbit j in M. $P_M(t)$ is the Poincaré polynomial of M, $(1-t^4)$ arises from the action of $SO(3)$ on M and $Q_V(t)$ is a series with non-negative coefficients. In the case of non-degenerate orbits (as guaranteed by morsification), the series $P_j(t)$ are found to be:

- $P_j(t) = 1$ for nonlinear configurations
- $P_j(t) = 1/(1-t^2)$ for collinear configurations.

Thus introducing M_n, m_n, the numbers of critical points with index n for nonlinear and collinear configurations, respectively, the Morse theory from Eqs. (1) and (2) takes the equivariant form on CS:

$$\sum_{i=0}^{3N-6} M_i t^i + \frac{\Sigma_{j=0}^{3N-5} m_j t^j}{1-t^2} = \frac{(1+2t^2)\cdots(1+(N-1)t^2)}{1-t^2} + (1+t)Q_V(t) \tag{3}$$

From Eq. (3), equating the coefficients of the same powers of t and considering that $Q_V(t)$ has only nonnegative coefficients, one gets explicitly the Morse inequalities on CS, the whole configuration space:

$$\begin{aligned}
M_0 + &\qquad m_0 \geqslant &&B_0^{(N)}\\
M_1 - M_0 + &\qquad m_1 - m_0 \geqslant &&-B_0^{(N)}\\
M_2 - M_1 + M_0 + &\qquad m_2 - m_1 + 2m_0 \geqslant &&B_1^{(N)} + 2B_0^{(N)}\\
M_3 - M_2 + M_1 - M_0 + &\qquad m_3 - m_2 + 2m_1 - 2m_0 \geqslant &&-B_1^{(N)} - 2B_0^{(N)}\\
M_4 - M_3 + M_2 - M_1 + M_0 + &\qquad m_4 - m_3 + 2m_2 - 2m_1 + 3m_0 \geqslant &&B_2^{(N)} + 2B_1^{(N)} + 3B_0^{(N)}
\end{aligned}$$

and

$$(-1)^{(3N-5)} m_{3N-5} + \cdots + m_2 - m_1 + m_0 = \frac{N!}{2} \tag{4}$$

The $B_i^{(N)}$ numbers are connected to the Betti numbers by the relation

$$B_i^{(N)} = \sum_{j=0}^{i} (-1)^{(i-j)} \beta_j^{(N)}$$

and one have Eq. (4a):

- for $N = 3$: $B_0^{(3)} = 1, \quad B_1^{(3)} = 2$
- for $N \geqslant 3$: $B_0^{(N)} = 1, \ldots, B_i^{(N)} = B_i^{(N-1)} + (N-1)B_{i-1}^{(N-1)}, \ldots, B_{N-2}^{(N)} = (N-1)B_{N-3}^{(N-1)}$

When exercising Eqs. (3) or (4), care is to be taken in determining the index of a critical point due to the "local dimension" of CS ($3N-5$ for collinear

configurations, $3N-6$ otherwise). Note also that a spatial critical configuration will count twice (mirror image) due to the reflexion not having been taken into account when defining CS as the quotient of M by $SO(3)$, rather than by $O(3)$. Symmetry-related configurations also have to be enumerated as illustrated in the following sections or elsewhere [5, 13–16].

3. Morse theory restricted to planar and collinear configurations

When restricting the study of some potential V to the linear plus planar configurations of a set of N nuclei, the planar configuration subspace (CSP) is everywhere $2N-3$ dimensional. Excising $D_{\text{excl.}}$ and contracting the translation as before, then taking advantage from the fact that the relevant rotational group S^1 acts freely, Palmore [14] derives the equivariant form of the Morse theory in this case as:

$$2\sum_{i=0}^{2N-3} M'_i t^i + \sum_{j=0}^{2N-3} m'_j t^j = \sum_{n=0}^{N-2} B_n^{(N)} t^n + (1+t)Q'_V(t) \tag{5}$$

where M'_n, m'_n are the number of planar critical configurations with index n on CSP (nonlinear and collinear resp.), $B_n^{(N)}$ as defined in Eq. (4a) and $Q'_V(t)$ has nonnegative coefficients. The factor 2 in the left hand side accounts for the reflexion of a nonlinear configuration with respect to a straight line [17]. Morse inequalities follow on CSP for k from 0 to $2N-3$:

$$\begin{aligned} &2(M'_k - M'_{k-1} + \cdots + (-1)^k M'_0) + m'_k - m'_{k-1} + \cdots + (-1)^k m'_0 \\ &\quad \geqslant B_k^{(N)} - B_{k-1}^{(N)} + \cdots + (-1)^k B_0^{(N)} \end{aligned} \tag{6}$$

where $B_k^{(N)} = 0$ for $k > N-2$ and the equality holds for $k = 2N-3$.

The case of collinear configurations (configuration subspaces CSL, $N-1$ dimensional) falls into the field of the Morse theory in its original form with Betti numbers $\beta_0 = 1$, $\beta_i = 0$ $i > 0$. There are $N!/2$ such subspaces imbedded in either CSP or CS, depending on the ordering of the labeled N nuclei along a straight line. For each of these subspaces, the Morse inequalities are for k from 0 to $N-1$:

$$m''_k - m''_{k-1} + \cdots + (-1)^k m''_0 \geqslant (-1)^k \tag{7}$$

where m''_0 stands for the number of critical points of index k for the restriction of V on the selected CSL and the equality holds for $k = N-1$.

The Equations (7) do not subsume in Eq. (6) which in turn, do not subsume in Eq. (4). However, a given critical configuration will appear at various places in these relations, depending on the partitioning of its unstable manifold (space spanned by the normal modes with imaginary frequencies) among the collinear planar and out-of-plane unstable modes. For example a collinear configuration with p collinear unstable modes and $2q$ other unstable modes in CS will account for m_{p+2q} in Eq. (4), m'_{p+q} in Eq. (6) and m''_p in Eq. (7). This reflects at the chemical level the properties of the flow of the gradient field issuing from some scalar and smooth potential function, i.e. the main foundations of both Morse and Catastrophe theories [2, 5, 18].

The following sections illustrate these main theorems in the case of Mg_n^+ or Mg_n^{++} clusters in their fundamental doublet or singlet states. The potential functions are derived from a non empirical model hamiltonian [19] fully invari-

ant with respect to any permutation among equivalent atoms and exhibiting various kinds of conical intersections and predissociative behaviors. Chemical intuition is meaningless for localisation of critical points with such fluxional systems. The algorithmic package available from AMPAC, version 2.1 [20] including the CHAIN method [21] and enlarged with simulated annealing strategies [22] to locate critical points of any index has been extensively used after implementation of the morsified potential function and its analytical molecular gradient.

4. 3-body cases

The "reduced configuration space" (RCS) of systems of 3 atoms can be spanned by the 3 Pekeris coordinates [23]. The RCS does not reflect the topology of CS, but the original Morse theory holds in RCS at the expense of raising the energy to a fix, constant, value at the boundary [10]. The following examples illustrate the difference between the two approaches in this case.

4.1. Cluster Mg_3^+

The cluster in its doublet ground state is a stable species with no predissociative behavior. However the potential needs morsification due to D_{3h} configurations (Jahn-Teller cusp) accounting for one pseudo critical point with index 2. Other critical points (Table 1) are the 3 equivalent $D_{\infty h}$ configurations (minima) and the 3 equivalent C_{2v} saddles. Thus on CS we have

$$m_0 = 3, \quad m_1 = 0, \quad m_2 = 0, \quad m_3 = 0, \quad m_4 = 0$$
$$M_0 = 0, \quad M_1 = 3, \quad M_2 = 1, \quad M_3 = 0$$

Table 1. Critical configurations of 3-atoms clusters. Potential functions from [19]. The label gives the local point group of symmetry, a "*" means morsification of a conical intersection, a "P" is for morsification of a dissociative channel. The energy of 3 neutral atoms is taken as reference. Geometries are the interatomic distances, most symmetric appearing first. The symmetry number is the number of equivalent but distinguishable configuration in CS. The index is for CS and leads to those in CSP or CSL by subtracting from it the relevant number of "frozen" unstable modes.

Cluster	Label	Energy (kcal/mol)	Geometry (Å)	Symmetry number	Index	Unstable modes
Mg_3^+						
	$D_{\infty h}$	132.71	3.062	3	0	
	$D_{3h}(*)$	142.76	1.925	1	2	E'
	C_{2v}	139.83	4.560, 2.995	3	1	B_1
Mg_3^{++}						
	$D_{\infty h}$	372.82	2.936	3	0	
	$C_{\infty v}$	378.07	5.687, 3.132	6	3	Σ^+, Π
	$C_{\infty v}(P)$	375.69	∞, 2.992	6	2	Π
	$D_{3h}(*)$	387.13	3.357	1	2	E'
	$D_{3h}(*)$	399.45	5.335	1	3	A', E'
	$D_{3h}(P,*)$	399.17	∞	1	2	E'
	$C_{2v}(P)$	369.10	∞, 2.971	3	0	
	C_s	377.19	3.000, 4.184, 6.271	6	1	A'

A 3-body configuration is necessarily planar and the same critical configurations appear on CSP, with the same indices in this case. Confining oneself to the linear configurations, one has on each of the 3!/2 CSL: $m_0 = 1$. The set of relations (4), (6), (7) is satisfied. In RCS, the original Morse theory is satisfied too, taking

$$M_0 = 3, \quad M_1 = 3, \quad M_2 = 1$$

due to the linear configurations which are stable with respect to bending.

4.2. *Cluster* Mg_3^{++}

This doubly charged ion does have stable forms but higher in energy than various channels leading to dissociated singly charged entities. Morsification regularizes the Jahn-Teller cusp (D_{3h} configurations) and converts long range repulsive valleys and ridges into ordinary critical points. The critical set (Table 1) can be classified in three subsets. Bounded subset: 3 equivalent $D_{\infty h}$ minima, 6 equivalent Cs scalene triangle (saddle) and 1 D_{3h} (index due to the Jahn–Teller cusp). Predissociative subset: 1 D_{3h} (index 3), 3 equivalent $C_{\infty v}$ (index 3 of which includes degenerate nonlinear unstable mode). Dissociative subset: $3C_{2v}$ isosceles triangle (minima) and 1 D_{3h} form (index 2) where both the regularization of the Jahn-Teller cusp and the penalization function are active. Collecting on CS:

$$m_0 = 3, \quad m_1 = 0, \quad m_2 = 6, \quad m_3 = 6, \quad m_4 = 0$$

$$M_0 = 3, \quad M_1 = 6, \quad M_2 = 2, \quad M_3 = 1$$

Nonlinear forms account similarly on CSP, but the nonlinear instability of the predissociated and dissociated $C_{\infty v}$ configurations leads to

$$m'_0 = 3, \quad m'_1 = 6, \quad m'_2 = 6$$

and the equivariant Morse relations Eqs. (3) and (5) are both satisfied. Note that in this case the inequalities Eq. (4) are less restrictive than of Eq. (6). Relations (7) on CSL are satisfied with $m''_0 = 2$ ($D_{\infty h} + C_{\infty v}$ dissociated) and $m''_1 = 1$. It is no longer possible to analyse the entire set of critical points in terms of the original Morse inequalities in RCS. However by compacifying the CS as proposed in [10] (see also appendix 2), one gets:

$$M_0 = 6, \quad M_1 = 6, \quad M_2 = 2, \quad M_3 = 1$$

The original Morse theory holds but the two $C_{\infty v}$ configurations must not be taken into account because they are unstable with respect to bending.

5. Applications to 4-body cases

With the increase in size, visual control on CS as a whole becomes impracticable. However, symmetry-constrained cross-sections become of major interest. Some critical point with an index of high value being found and playing a central role, it is also very efficient to look at the other critical points surrounding the central one. The original Morse theory applies on the manifold (unstable manifold) spanned by the gradient trajectories descending from the central point. This provides an efficient strategy for prospection on the potential [7, 8]. Controls of topological consistency follow on larger and larger cross-sections of CS. Of course the strategy applies in turn on CSP and CSL.

5.1. Cluster Mg_4^+

Like Mg_3^+ cluster, Mg_4^+ is a stable species. The threefold crossing at T_d configurations and the issuing twofold conical intersections need morsification (see [16] for a generic study of such structures). The entire set of critical points belongs to the unstable manifold of a Td pseudo-critical point. This illustrates the decisive importance of critical points of high indices in the main organization of potential surfaces. Results are summarized in Table 2, except a local set of 4 connected critical points, with very closed geometries and energies, which can be collapsed onto no critical point by the contraction method [5, 18]: one $C_{2v}^{(4,2,2)}$ (conical intersection, index 3), one $C_{2v}^{(4,2,2)}$ (index 1), two equivalent $C_s^{(4)}$ (index 2), with energies 136.47 ± 0.14 kcal/mol. Most of the critical points lie in either the C_2 or $C_s^{(2)}$ symmetry-constrained cross-sections of the unstable manifold of T_d. They are always stable with respect to the extensive coordinates (hyper radius), thus allowing 3-D representations (Figs. 1 and 2) after removal of this contractible degree of freedom. Original Morse theory applies on these

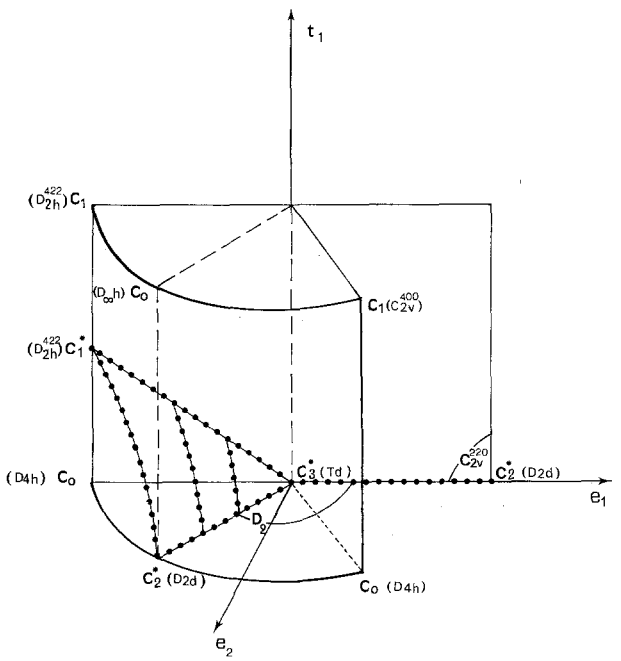

Fig. 1. C_2 cross-section of the unstable manifold of a T_d configuration for Mg_4^+ cluster. At the origin, one finds the T_d (Jahn–Teller) configuration with pseudo-index 3 in this cross-section. The horizontal plane, spanned by the E modes, is also the D_2 cross-section embedding the 3 D_{2d} cross-sections which correlate with planar configurations D_{4h}. The proper T_2 mode spans the vertical axis such that the vertical plane (e_1, t_1) is the cross-section of symmetry $C_{2v}^{(2,2,0)}$ which correlates with planar configurations $D_{2h}^{(4,0,0)}$. The unstable manifold propagates also up to $C_{2v}^{(4,0,0)}$ (planar) and $D_{\infty h}$ (linear) configurations. The conical intersections (solid circles) due to Jahn–Teller crossing at T_d point are either one-dimensional (right-half axis e_1) or 2-D (cone around left-half axis e_1). The entire figure is of C_{2v} symmetry and for completeness requires reflexions with respect to horizontal D_2 plane and vertical $C_{2v}^{(2,2,0)}$ plane. The cylinder is for visual convenience. Critical points are labeled as in Table 2.

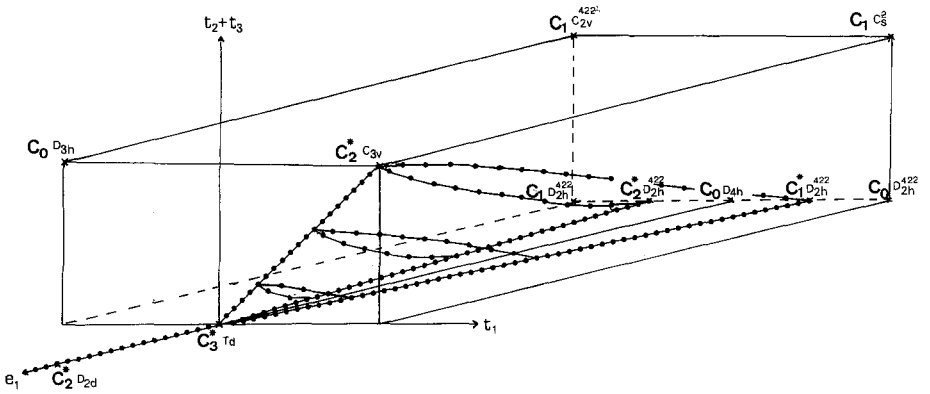

Fig. 2. $C_s^{(2)}$ cross-section of the unstable manifold of a T_d configuration for Mg_4^+ cluster. The horizontal plane is the $C_{2v}^{(2,2,0)}$ cross-section (vertical plane in Fig. 1). The vertical axis is the proper T_2 mode which, in conjunction with $t1$, spans the C_{3v} cross-section which correlates with D_{3h}. Conical intersections (solid circles) are centered around the $e1$ axis: 1-D on the left, 2-D on the right. The horizontal plane acts as a reflexion plane for completeness. The parallelepiped is for visual convenience. Other notations as in Fig. 1

sub-manifolds with the homotopy of $\mathscr{R}^3$, and actual counts:

$$M_0 = 7, \quad M_1 = 8, \quad M_2 = 3, \quad M_3 = 1 \quad \text{on } C_2$$

$$M_0 = 4, \quad M_1 = 6, \quad M_2 = 4, \quad M_3 = 1 \quad \text{on } C_s^{(2)}$$

All the planar critical configurations have only a stable out-of-plane mode. Scanning Table 2, we collect on CSP:

$$M_0' = M_0 = 7, \quad M_1' = M_1 = 36, \quad M_2' = M_2 = 24, \quad m_0' = m_0 = 12$$

Table 2. Critical points of Mg_4^+ cluster. Col. 1, the figures in parentheses give the number of atoms located on an element of symmetry: $D_{2h}(\sigma, \sigma, \sigma)$, $C_{2v}(\sigma_v, \sigma_v', C_2)$. Other notations as in Table 1. The last two columns give the index of the critical points when restricted into C_2 (Fig. 1) and $C_s^{(2)}$ (Fig. 2) cross-sections issuing from T_d

Mg_4^+ Label	Energy (kcal/mol)	Symmetry number	Index	Unstable modes	C_2	$C_s^{(2)}$
Linear						
$D_{\infty h}$	124.83	12	0		0	
Planar						
D_{4h}	127.43	3	0		0	0
D_{3h}	124.67	4	0			0
$D_{2h}^{(4,2,2)}$	133.90	6	2	B_{1g}, B_{2u}	1	0 or 1
$D_{2h}^{(4,2,2)}(*)$	134.56	6	2	A_g, B_{2u}	1	1 or 2
$C_{2v}^{(4,2,2)}$	127.89	12	1	A_1		1
$C_{2v}^{(4,0,0)}$	128.66	12	2	A_1, B_1	1	
$C_s^{(4)}$	127.78	24	1	A'		
Spatial						
$T_d(*)$	139.68	2	5	E, T_2	3	3
$C_{3v}(*)$	137.78	8	4	$2E$		2
$D_{2d}(*)$	138.18	6	4	B_1, B_2, E	2	2
$C_s^{(2)}$	137.10	24	3	$A', 2A''$		1

and inequalities of Eq. (6) with $B_0 = 1$, $B_1 = 5$, $B_2 = 6$ are satisfied. Taking into account the non-planar critical points, one gets

$$M_3 = 24, \quad M_4 = 14, \quad M_5 = 2$$

which in turn give for inequalities (4) on CS:

$$\begin{aligned}
7 + & \qquad 12 = 19 \geqslant & 1 \\
36 - 7 + & \qquad 0 - 12 = 17 \geqslant & -1 \\
24 - 36 + 7 + & \qquad 0 - 0 + 2 \times 12 = 19 \geqslant & 7 \\
24 - 24 + 36 - 7 + & \qquad 0 - 0 + 0 - 2 \times 12 = 5 \geqslant & -7 \\
14 - 24 + 24 - 36 + 7 + & \qquad 0 - 0 + 0 - 0 + 3 \times 12 = 21 \geqslant & 19 \\
2 - 14 + 24 - 24 + 36 - 7 + & \qquad 0 - 0 + 0 - 0 + 0 - 3 \times 12 = -19 \geqslant & -19
\end{aligned}$$

5.2. *Cluster* Mg_4^{++}

This species accumulates the difficulties of both Mg_3^{++} and Mg_4^{+} clusters. This hyper-radius is not contractible due to predissociative behavior. Conical intersections not only propagate from T_d, but also are encountered in various planar forms. With respect to previous clusters, the increase in the number of critical points is formidable, some of them being of low symmetry (or none). However, simulated annealing methods turn out to be very fruitful in the location of critical points of any index, with or without symmetry constraints. Driving the search as proposed at the beginning of this section, there are no difficulties in locating the 921 critical points of the singlet ground state of this cluster (Table 3). Morse theory is satisfied not only on CSL, CSP and CS but also on each of the symmetry-constrained cross-sections of the unstable manifold of critical points with major symmetry (T_d, D_{4h}).

Contrary to previous clusters, most of linear configurations are unstable with respect to bending. The role of the penalization function raising up at large values of the total inertia is illustrated on CSL which is three dimensional (Fig. 3).

The $D_{\infty h}$, D_{4h} and $D_{2h}^{(4,0,0)}$ cross-sections are embedded in the $C_{2v}^{(4,0,0)}$ one, spanned by three internal coordinates (Fig. 4). Two coordinates are bond lengths in nature, the third being angular and periodic. Selecting from Table 3 the critical points with D_{4h} and $D_{2h}^{(4,0,0)}$ symmetry, one builds up a 2-D cross-section. The relevant $D_{\infty h}$ critical points give another one. Then collecting in turn the $C_{2v}^{(4,0,0)}$ critical points and continuing until the period of the angular variable is reached, and global count in one period takes the form:

$$\begin{aligned}
M_0 = 6: \quad & 2D_{4h} && + 4D_{2h}^{(4,0,0)}(P) && \\
M_1 = 12: \quad & && 4D_{2h}^{(4,0,0)} && + 8D_{\infty h}(P\colon A, B, C, D) \\
M_2 = 8: \quad & 2D_{4h}(P) && && + 2D_{\infty h}(P\colon E) && + 4C_{2v}^{(4,0,0)} \\
M_3 = 2: \quad & 2D_{4h} && && &&
\end{aligned}$$

in accordance with Morse theory on the torus (Betti numbers $\beta_0 = 1$, $\beta_1 = 1$, $\beta_2 = 0$ [3, 4]).

Table 3a

Mg_4^{++} Label	Energy (kcal/mol)	Symmetry number	Index			Unstable modes
			CS	CSP	CSL	
Linear						
$D_{\infty h}$:						
$A(P)$	321.43	12	4	2	0	Π_g, Π_u
$B(P)$	361.16	12	5	3	1	Σ_u^+, Π_g, Π_u
C	367.31	12	4	3	2	$\Sigma_g^+, \Sigma_u^+, \Pi_g$
$D(P)$	368.86	12	2	2	2	Σ_g^+, Σ_u^+
E	368.91	12	3	3	3	$2\Sigma_g^+, \Sigma_u^+$
$C_{\infty v}$:						
(P)	334.44	24	2	1	0	Π
(P)	344.93	24	3	2	1	Σ^+, Π

Table 3b

Mg_4^{++} Label	Energy (kcal/mol)	Symmetry number	Index			Unstable modes
			CS	CSP	CSL	
Planar						
D_{4h}:						
	342.84	3	0	0		
(P)	377.45	3	4	4		B_{1g}, B_{2g}, E_u
	382.70	3	5	5		$A_{1g}, B_{1g}, B_{2g}, E_u$
D_{3h}:						
	347.55	4	0	0		
(P)	377.42	4	2	2		E'
	380.77	4	5	5		$A_1', 2E'$
$D_{2h}^{(4,2,2)}$:						
(P)	358.11	6	2	1		B_{1u}, B_{2u}
	372.31	6	4	4		$A_g, B_{1g}, B_{2u}, B_{3u}$
	378.15	6	4	4		$A_g, B_{1g}, B_{2u}, B_{3u}$
(*)	378.25	6	5	5		$2A_g, B_{1g}, B_{2u}, B_{3u}$
$D_{2h}^{(4,0,0)}$:						
(P)	318.77	6	1	0		B_{1u}
	344.25	6	1	1		A_g
C_{2h}:						
	367.30	12	2	2		A_g, B_u
$C_{2v}^{(4,0,0)}$:						
	358.56	12	3	3		$2A_1, B_1$
$C_{2v}^{(4,2,2)}$:						
(P)	319.93	12	2	1		B_1, B_2
(P)	332.24	12	0	0		
(P)	338.82	12	2	1		B_1, B_2
(P)	340.40	12	2	1		B_1, B_2
$(P, *)$	342.49	12	3	2		A_1, B_1, B_2
$(P, *)$	342.63	12	4	3		$A_1, 2B_1, B_2$
(P)	344.22	12	1	1		A_1
(*)	355.67	12	2	2		A_1, B_1

Table 3b (continued)

Mg_4^{++} Label	Energy (kcal/mol)	Symmetry number	Index			Unstable modes
			CS	CSP	CSL	
	356.88	12	1	1		A_1
	357.59	12	2	2		A_1, B_1
	358.33	12	2	2		A_1, B_1
	359.21	12	3	3		$2A_1, B_1$
	369.01	12	3	3		$A_1, 2B_1$
(*)	369.42	12	4	4		$2A_1, 2B_1$
	380.40	12	4	4		$2A_1, 2B_1$
	380.41	12	4	4		$2A_1, 2B_1$
$C_s^{(4)}$:						
	355.58	24	1	1		A'
	358.04	24	2	2		$2A'$
	364.46	24	2	2		$2A'$
	367.05	24	4	3		$3A', A''$

Table 3(a–c). Critical points of Mg_4^{++} cluster. The capital letters in col. 1 refer to symbols in Figs. 3 and 4. Notations as in Table 2; $C_s(\sigma)$ indicates the number of atoms of the σ plane. The various indices refer to configuration spaces as defined in text

Mg_4^{++} Label	Energy (kcal/mol)	Symmetry number	Index			Unstable
			CS	CSP	CSL	
Spatial						
T_d:						
(*)	362.92	2	2			E
(*P*, *)	381.59	2	3			T_2
(*)	391.93	2	6			A_1, E, T_2
C_{3v}:						
(*P*, *)	341.99	8	4			$2E$
(*)	365.64	8	5			$A_1, 2E$
(*)	369.83	8	5			$A_1, 2E$
D_{2d}:						
(*P*)	318.73	6	0			
$C_s^{(2)}$:						
	338.75	24	2			A', A''
C_1:						
	345.72	48	1			
	352.08	48	2			
	359.26	48	2			
	359.37	48	3			
	366.51	48	3			
	374.29	48	3			
	375.83	48	3			
	381.93	48	5			

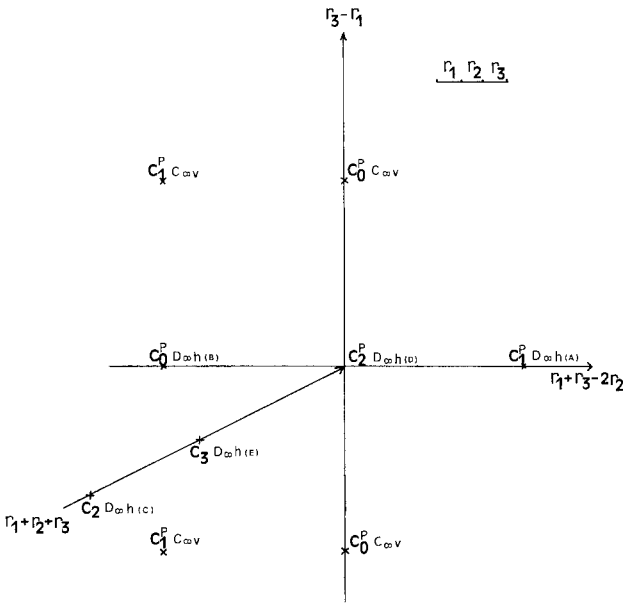

Fig. 3. Linear critical set of Mg_4^{++} cluster (singlet ground state). The $D_{\infty h}$ cross-section is the horizontal plane, acting also as a reflexion plane of the entire figure. The penalty function suddenly rises up at large values of the extensive coordinate and converts dissociative channels and ridges into ordinary critical points (bottom vertical plane). Other notations in accordance with Table 3.

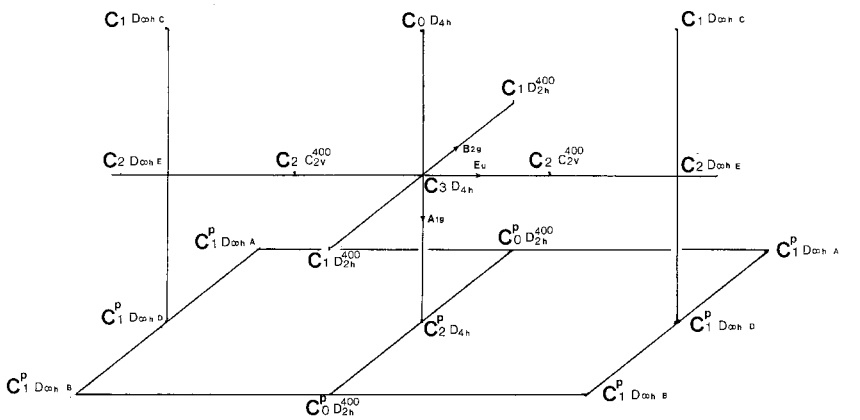

Fig. 4. Half-period of a $C_{2v}^{(4,0,0)}$ cross-section of Mg_4^{++} cluster. The A_{1g}, B_{2u}, E_u (periodic) modes of the central D_{4h} configuration (index 3) span the entire figure. Penalization is reached at large values of the A_{1g} mode (bottom horizontal plane). The $D_{2h}^{(4,0,0)}$ cross-section embedding the D_{4h} one lies on the centered vertical plane. The left vertical plane is the $D_{\infty h}$ cross-section also shown in Fig. 3. The right vertical plane is equivalent to the left one, differing only by permutation among equivalent nuclei

There are six such distinguishable $C_{2v}^{(4,0,0)}$ cross-sections on CSP, sharing two by two the D_{4h} and $D_{2h}^{(4,0,0)}$ critical points (recall that on CSP, nonlinear configurations are doubled in count, the linear being not). A similar property has been observed elsewhere [16]: a given critical point, shared between equivalent cross-sections, distributes its modes belonging to distinct irreducible representations in a non symmetric way. However the overall symmetry is kept, due to another equivalent critical point shared in the opposite way.

6. Conclusion

The knowledge of the set of critical points of a potential function gives information about its intrinsic complexity. Of course complexity tends to increase with N, the number of atoms, as indicated by equivariant Morse theory (the number of critical point grows usually faster than $N!$ [13]). However, for a given value of N, there exist more or less simple surfaces too. For example, let us take as a criterion the distribution of the energies of the critical points with a given index. These distributions can in turn be summarized by their mean values and standard deviations (Table 4).

The surface of Mg_3^+ is one of the simplest possible with no overlap in the distributions of various indices. A greater complexity is apparent for Mg_3^{++} from the overlap between distributions of indices 1 and 2. In spite of the increase in the number of critical points, the surface of Mg_4^+ is simple. On the other hand, the surface of Mg_4^{++} is a complicated one, with strong overlap between the distribution of non-contiguous indices.

Let us suppose that some properties are needed which involve trajectories on these surfaces (either from molecular dynamics or Metropolis scheme). A problem is to build up a good sampling of the configuration space. Of crucial importance to provide answers is the branching tree of connected components i.e. the energetic levels where separated basins collapse. The levels where "holes" in a connected component disappear are also useful. Such information is roughly summarized in the energetic distributions of critical points with specified index as illustrated in Table 4.

Global analysis of a potential energy function is of decisive importance for the understanding – at least qualitative – of a potential hypersurface in chemistry [10]. The location of critical points requires an efficient arsenal of optimizations methods, including both local and non-local algorithms, hessian matrix analysis and integration of gradient trajectories [20–22]. However, faced with the

Table 4. Mean value $\bar{E}$ and standard deviation σ of the energies (kcal/mol) of the critical points of some clusters of Mg_n in their ground states. M is the number of critical points for a given index

Index:	0	1	2	3	4	5	6
Mg_3^+							
M	3	3	1				
$\bar{E}$	132.71	139.83	142.76				
σ	—	—	—				
Mg_3^{++}							
M	6	6	8	7			
$\bar{E}$	370.96	377.19	380.05	381.12			
σ	1.89	—	8.13	7.48			
Mg_4^+							
M	19	36	24	24	14	2	
$\bar{E}$	125.21	127.82	131.44	137.10	137.95	139.68	
σ	0.96	0.11	2.79	—	0.19	—	
Mg_4^{++}							
M	25	108	300	278	119	89	2
$\bar{E}$	332.72	347.41	352.36	364.99	362.35	376.30	391.93
σ	9.73	8.56	11.85	9.20	18.36	8.03	—

complexity of potential functions, a crude use of these methods will usually lead to sparse information, with no topological consistency.

Fortunately, Morse theory provides an elegant and powerful framework for rationalization of numerical results. In previous works [7–11, 15, 16] this was done on various subsets of the configuration space and in conjunction with symmetry. The present work enlarges the field of applicability of Morse theory to the configuration space as a whole and its restrictions to planar and linear cases. The various forms of Morse theory thus provide very severe tests for topological consistency, in a way which evolves from semi-local analysis to global analysis.

When exercising such an analysis, several pitfalls can be encountered due to the potential arising from the diagonalization of some hamiltonian matrix. Systematizing the use of penalty function [15], generic perturbation [16] or Catastrophe theory [5, 18] we propose a rational way to achieve morsification of potential function, without loss of the main chemical significance attached to these surfaces.

7. Appendices

1. Morsification of potential functions

When a potential function shows a repulsive behavior at large distances, Morse theory does not apply since condition (ii) is not satisfied whatever boundary chosen. The "Palais–Smale" condition (see [5], and [10] p. 78) is restored by introducing a penalty function at large distances: this converts a repulsive valley (ridge) into an ordinary minimum (critical point) [15]. Let some hyperspherical coordinates system span CS. The hyper-radius (or equivalently the total inertia I of the system) is the only extensive coordinate, thus increasing along any path of fragmentation of the system. Therefore a penalty function P converting the original potential V into a distorted one W can be defined as:

$$I < I_0 \Rightarrow P = 0$$

$$I \geqslant I_0 \Rightarrow P = k(I - I_0)^3$$

$$W = V + P$$

where k is a constant with a positive value and I_0 a large enough threshold value on the total inertia. The power three ensures differentiability up to second order for analytical computation of the hessian everywhere. This penalty function is not so elegant as the "carpeted step functions" ([10] p. 273) but it is much easier for numerical implementation. Critical points of W do exist in the vicinity of the border $I - I_0$, which reflect at finite distance the dissociative behavior of V. These critical points have an obvious chemical significance and they account for Morse theory ([2] Theorem 1.4, p. 145).

First-order discontinuities induced by conical intersections or Jahn–Teller cusps generate pseudo-critical points with pseudo-index as proposed in Ref. [16]. Let O be the subspace where the eigenstates split in first order and T be the complementary subspace. A pseudo-critical point does exist if and only if the potential function is at a critical value on T and if its left and right derivatives are of opposite signs on O. Then, for the lowest adiabatic eigenstate, the pseudo-index is the sum of the index on T plus the dimensionality of O. This

regularization can be extended to excited states, with the results depending on both the parity of the state and the number of simultaneous crossings. The last kind of difficulty comes from degenerate critical points. Mathematically, this is a non-generic situation, i.e. rare and unstable under most perturbations. How an isolated critical point bifurcates into non degenerate critical points under a given perturbation is described in the Catastrophe theory [18]. Notwithstanding the perturbation, Morse theory applies to each of the reachable generic situations. As an example, the two-dimensional "monkey-saddle" case [24] is a catastrophe germ D-4 separating three generic situation: (1 minimum, 3 saddles), (2 saddles), (1 maximum, 3 saddles). The actual choice does not affect the chemical significance of the potential function. Going further, such conventional perturbations apply to subsets of connected critical points using the fold contraction technique. This provides a powerful tool either to describe the gross properties of a potential function [8] or to reduce the complexity of a local set of critical points as illustrated in this work in the case of Mg_4^+.

2. *On the compacification of configuration spaces* (CS)

In the original work of M. Morse ([2], Theorem 1.1, p. 143), the inequalities are derived in a compact manifold. However, the CS is not a compact but it may be compacified. P. Mezey [10] actually proposes to convert the CS into a "manifold with boundary" (p. 270). Then the potential function is distorted near the boundary by raising the energy to a large enough value (p. 289). Finally, the boundary is contracted to a single point (p. 286). This completes the compacification and introduces an additional, artificial maximum point. This last step is not necessary because Morse theory holds in open sets if the potential function satisfy a "Palais–Smale" condition [5]. It actually does by raising the energy near the boundary ([2] Theorem 1.2, p. 145).

In the three-body case, linear configurations lie on the boundary ([10], p. 272). When raising the energy, linear critical points remain if the bending mode is stable, but they disappear if not. Therefore a chemical information is lost in some sense. This is disappointing when most of the critical configurations are collinear (e.g. CO_2).

The deficiency remains in the four-body case while other obstacles appear. The "reduced configuration space" (RCS) is defined as a metric space, of dimension $3N-6=6$ ([10], p. 26). To build up a manifold with boundary, one has to define a simply connected boundary of dimension 5. In order to avoid the reflexion properties ([10], p. 219), the set of collinear configurations has to belong to this boundary, but its dimension is only 3. The set $D_{\text{excl.}}$ of superimposed nuclei, to be excluded, must also belong to the boundary. However, the set $D_{\text{excl.}}$ is not fully included in the set of collinear configurations and some of its components are of dimension lower than 5. How to imbedd these various boundary sets in a unique boundary, without breaking the RCS into disjoint subsets, is an open question.

Also not evident that rotational equivalences can be eliminated everywhere while building up a Riemannian space as defined in [2], chapter V. For example, with four atoms A, B, C, D, and six cartesian coordinates (none for A, one for B, two for C and three for D, similarly to [10] page 271), the atom D can rotate freely around the ABC axis when these first three atoms are in a straight line. The problem occurs for planar configurations but not for linear ones. The use of

another system of $3N-6$ independent coordinates displaces the problem but does not remove it in the large. P. Mezey ([10] chapter V) clearly shows that the RCS can be endowed with a metric. We have not been able to prove that it is sufficient in the sense of Morse ([2] chapter V).

The complexity of the RCS emerges at four atoms. Unfortunately, obstacles increase with the number of atoms. For example, a natural (although chemically frustrating) boundary in a four-body case may be provided by the set of planar configurations. This is no longer true for a system with five atoms where the set of planar configurations is of dimension 7 versus a RCS of dimension 9. Instead of attempting to compacify, another approach is first to solve the problem of superimposed nuclei in the $\mathscr{R}^{3N}$ space, as done since 1962 [12]. Then one can decide to keep linear and planar configurations within the "interesting" part of CS in chemistry. At least the problem of rotational equivalences can be entered, even if the CS fails to be a manifold, at the expense of computing once for all non-trivial topological invariants, in the spirit of [13].

References

1. Born M, Oppenheimer JR (1927) Ann Phys 84:457
2. Morse M (1934) Calculus of variation in the large. Am Math Soc Colloquium Pub 18
3. Spanier EG (1966) Algebraic topology, McGraw Hill, NY
4. Greenberg M (1966) Lectures on algebraic topology. Benjamin, NY
5. Palais RS (1970) Critical point theory and the minimax principle. Global Analysis. Proc. Sym Pure Math 15:198 A.M.S. Providence
6. Mezey PG (1988) Chem Phys Lett 82:100; 86:562 (1982)
7. Liotard D (1979) Thesis, Pau
8. Liotard D (1983) In: (eds. Maruani, Serre) Symmetries and properties of non-rigid molecules, p. 323, Elsevier, NY; Iratcabal P, Liotard D (1988) J Am Chem Soc 110:4919
9. Peterson MR, Gsizmadia IG, Sharpe RW (1983) J Mol Struct (Theochem) 94:127
10. Mezey PG (1987) Potential energy hypersurfaces, Elsevier, NY
11. Mezey PG (1980) Theor Chim Acta 54:95
12. Fadell E, Neuwirth L (1962) Math Scand 10:111
13. Pacella F (1987) Arch. rat. Mech. Anal. 97:59
14. Palmore JI (1976) Lett Math phys 1:119 and ref. therein
15. Cardy H, Dargelos A, Liotard D, Poquet E (1983) Chem Phys 77:287
16. Liotard D, Roche M (1987) J Comp Chem 8:850
17. Pacella F (1986) Trans Am Math Soc 297:41
18. Gilmore R (1981) Catastrophe theory for scientists and engineers, Wiley, NY
19. Durand G (1989) J Chem Phys 91:6225
20. AMPAC, version 2.1, Dewar research group, University of Texas at Austin, 78715 Austin (TX)
21. Liotard D, Penot JP (1981) In: (ed. Della-Dora), Numerical methods in the study of critical phenomena, p 213, Springer, Berlin Heidelberg New York; Liotard D (1992) Int J Quant Chem 44:723
22. Bockisch F, Liotard D, Rayez JC, Duguay B (1992) Int J Quant Chem 44:619
23. Davidson E. R (1977) J Am Chem Soc 99:397
24. Mezey P. G (1977) In: (ed. Czismadia), Applications of M.O. theory in organic chemistry, p 127, Elsevier